Supplementary Material

All-or-none Suppression of B Cell Terminal Differentiation by Environmental Contaminant 2,3,7,8-Tetrachlorodibenzo-p-Dioxin

Qiang Zhang, Douglas E. Kline, Sudin Bhattacharya, Robert B. Crawford, Rory B. Conolly, Russell S. Thomas, Melvin E. Andersen, and Norbert E. Kaminski

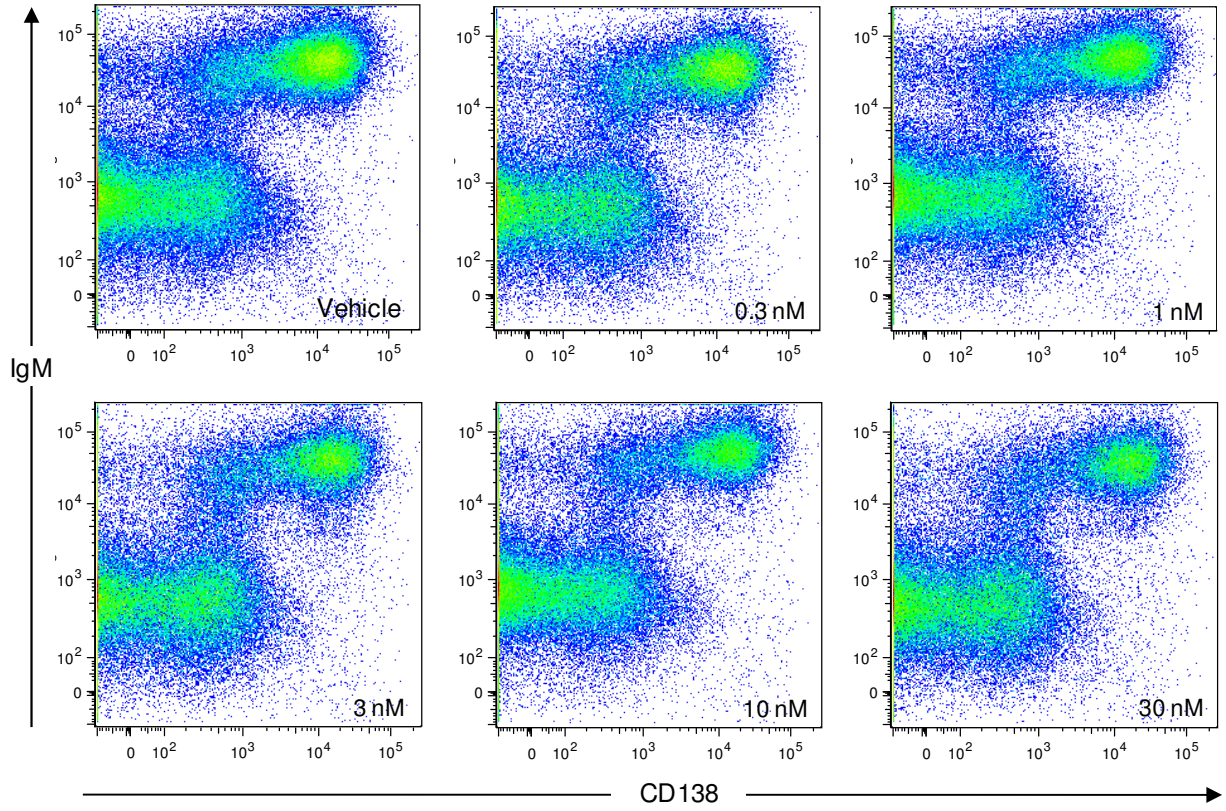

Figure S1. Flow cytometry analysis showing co-expression of intracellular IgM and surface marker CD138 in CD19-gated primary mouse B cells stimulated with 5 μg/ml LPS for 72 h in the absence or presence of various concentrations of TCDD as indicated.

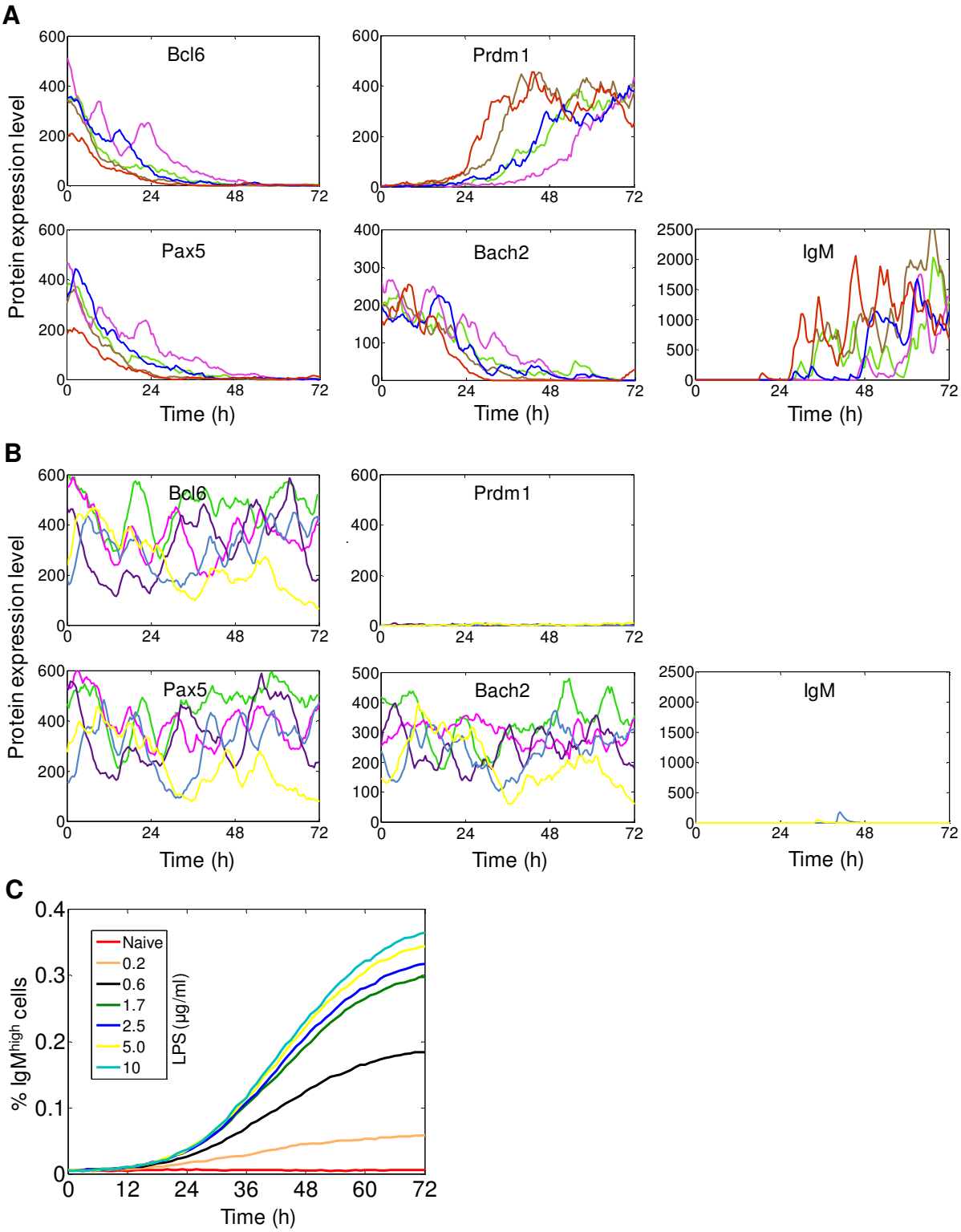

Figure S2. Protein expression and cell population dynamics of stochastically-simulated B cells under continuous LPS stimulation. (A) Trajectories of five simulated cells en route to switching to IgM^{high} cells under continuous stimulation by 5 μg/ml LPS for 72 h. In the course of this switching process, Bcl6, Pax5, and Bach2 genes are turned off, while Prdm1 and IgM genes are turned on. **(B)** Trajectories

of five simulated cells that do not respond to stimulation by 5 μg/ml LPS for 72 h, illustrating probabilistic switching. For these non-responsive cells, expression levels of Bcl6, Pax5, and Bach2 remain high, while Prdm1 and IgM remain low. **(C)** Stochastic simulations of 20,000 B cells continuously stimulated by various concentrations of LPS for 72 h. The responses show that IgM^{high} cells accumulate at a rate positively correlating with LPS concentration.

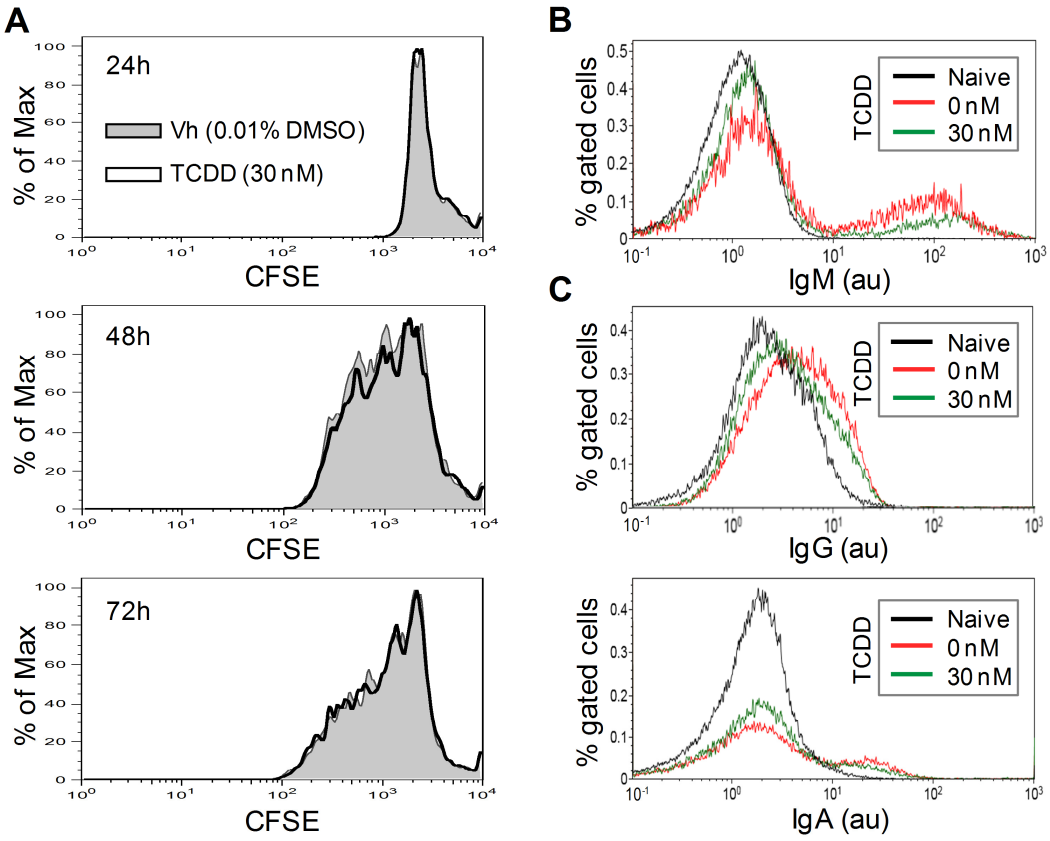

Figure S3. Effects of TCDD on B cell proliferation, kinetics of the IgM response, and IgG- and IgA-producing cells. Primary mouse splenocytes were simultaneously treated with 5 μg/ml LPS and with TCDD (30 nM) or vehicle (0.01% DMSO). **(A, left panels)** Cell proliferation was evaluated by using CSFE staining measured by flow cytometry at 24, 48 and 72 h post LPS activation. Shaded histogram: vehicle (Vh), empty histogram with bold tracing: TCDD (30 nM). The two histograms essentially overlapped, indicating that TCDD did not alter cell proliferation. **(B, top right panel)** Intracellular IgM staining on Day 5 post LPS activation ruled out the possibility that the suppressed IgM response by TCDD observed on Day 3 (Fig. 5B) was simply due to a shift of the kinetics of the IgM response because no higher response was observed beyond Day 3 (measured on Day 5 here) in the presence of TCDD. **(C, middle right and bottom right panels)** Intracellular IgG and IgA staining measured by flow cytometry on Day 3 post LPS activation showed that TCDD did not promote the formation of IgG- or IgA-secreting cells. This result ruled out the possibility that the TCDD-mediated IgM suppression was due to increased differentiation of B cells into other antibody isotype-producing cells.

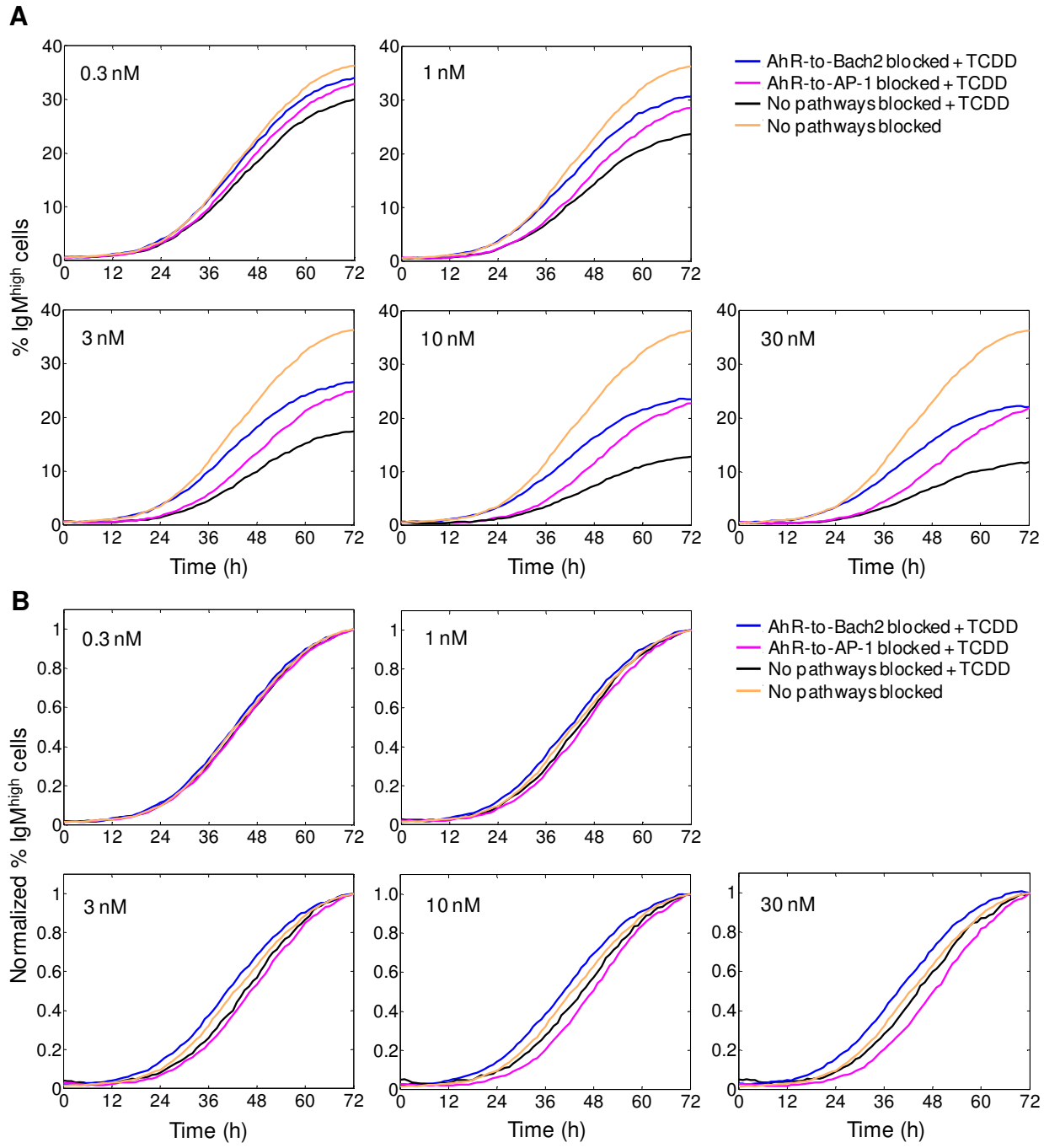

Figure S4. Comparison of the effects of AhR-mediated AP-1 and Bach2 pathways on the B cell differentiation response. (A) Blocking either the AhR-to-AP-1 or AhR-to-Bach2 pathway (pink and blue curves respectively) recovers the IgM^{high} cell response suppressed by TCDD to a comparable extent at 72 h. Black curves: neither of the two pathways blocked. Orange curves: neither of the two pathways blocked and no TCDD. All simulation results were obtained with 20,000 stochastically simulated B cells continuously exposed to 10 μg/ml LPS and various concentrations of TCDD except for the orange curves, which were obtained in the presence of 10 μg/ml LPS only. Blockade of activation of Bach2 by TCDD was realized by setting parameter a_{71}=0 and blockade of inhibition of AP-1 by TCDD was realized by setting parameter kd_{31}=2.5e8. **(B)** Normalization of the responses from panel A shows that when acting primarily through the Bach2 pathway (i.e. AhR-to-AP-1 pathway blocked, pink curves), TCDD introduces a time

delay in the differentiation response of B cells compared with acting primarily through the AP-1 pathway (i.e., AhR-to-Bach2 pathway blocked, blue curves).

Table S1. Ordinary differential equations (ODEs) and initial values of the computational model

Variable name	ODE	Initial value	Note
$Bcl6\_GENE_1$	$\frac{d(Bcl6\_GENE_1)}{dt} = -(k_{00} + \frac{k_{01} \cdot Prdm1}{Kd_{01} + Prdm1}) \cdot Bcl6\_GENE_1 + k_{02} \cdot (Bcl6\_GENE_{tot} - Bcl6\_GENE_1)$	0.22	Active Bcl6 gene
$Bcl6\_mRNA$	$\frac{d(Bcl6\_mRNA)}{dt} = k_{03} \cdot Bcl6\_GENE_1 - k_{04} \cdot Bcl6\_mRNA$	48	Bcl6 mRNA
$Bcl6$	$\frac{d(Bcl6)}{dt} = k_{05} \cdot Bcl6\_mRNA - k_{06} \cdot Bcl6$	300	Bcl6 protein
$Prdm1\_GENE_1$	$\frac{d(Prdm1\_GENE_1)}{dt} = -k_{11}(\frac{a_{11} \cdot Pax5}{Kd_{11} + Pax5} + \frac{a_{12} \cdot Bach2}{Kd_{14} + Bach2}) \cdot Prdm1\_GENE_1$ $+ (k_{10} + k_{12} \cdot \frac{AP1p}{Kd_{13} + AP1p} \cdot \frac{Kd_{12}}{Kd_{12} + Bcl6}) \cdot (Prdm1\_GENE_{tot} - Prdm1\_GENE_1)$	0.005	Active Prdm1 gene
$Prdm1\_mRNA$	$\frac{d(Prdm1\_mRNA)}{dt} = k_{13} \cdot Prdm1\_GENE_1 - k_{14} \cdot Prdm1\_mRNA$	0.32	Prdm1 mRNA
$Prdm1$	$\frac{d(Prdm1)}{dt} = k_{15} \cdot Prdm1\_mRNA - k_{16} \cdot Prdm1$	1	Prdm1 protein
$Pax5\_GENE_1$	$\frac{d(Pax5\_GENE_1)}{dt} = -(k_{20} + \frac{k_{21} \cdot Prdm1}{Kd_{21} + Prdm1}) \cdot Pax5\_GENE_1 + k_{22} \cdot (Pax5\_GENE_{tot} - Pax5\_GENE_1)$	0.22	Active Pax5 gene
$Pax5\_mRNA$	$\frac{d(Pax5\_mRNA)}{dt} = k_{23} \cdot Pax5\_GENE_1 - k_{24} \cdot Pax5\_mRNA$	48	Pax5 mRNA
$Pax5$	$\frac{d(Pax5)}{dt} = k_{25} \cdot Pax5\_mRNA - k_{26} \cdot Pax5$	300	Pax5 protein
$Bach2\_GENE_1$	$\frac{d(Bach2\_GENE_1)}{dt} = -k_{71} \cdot Bach2\_GENE_1$ $+ k_{72} \cdot \frac{Pax5}{Kd_{71} + Pax5} \cdot (1 + a_{71} \cdot \frac{TCDD\_AhR}{Kd_{72} + TCDD\_AhR}) \cdot (Bach2\_GENE_{tot} - Bach2\_GENE_1)$	0.175	Active Bach2 gene
$Bach2\_mRNA$	$\frac{d(Bach2\_mRNA)}{dt} = k_{73} \cdot Bach2\_GENE_1 - k_{74} \cdot Bach2\_mRNA$	38	Bach2 mRNA
$Bach2$	$\frac{d(Bach2)}{dt} = k_{75} \cdot Bach2\_mRNA - k_{76} \cdot Bach2$	240	Bach2 protein
$AP1$	$\frac{d(AP1)}{dt} = k_{31} \cdot \frac{Kd_{31}}{Kd_{31} + TCDD\_AhR} - k_{32} \cdot AP1 + k_{33} \cdot AP1p - (k_{34} + k_{35} \cdot LPS\_TLR4) \cdot AP1$	400	Unphosphorylated AP-1

$AP1p$	$\frac{d(AP1p)}{dt} = -k_{33} \cdot AP1p + (k_{34} + k_{35} \cdot LPS\_TLR4) \cdot AP1 - k_{36} \cdot AP1p$	100	Phosphorylated AP-1
$TCDD\_AhR$	$\frac{d(TCDD\_AhR)}{dt} = k_{41} \cdot TCDD \cdot (\ AhR_{tot} - TCDD\_AhR\ ) - k_{42} \cdot TCDD\_AhR$	0	TCDD-occupied AhR
$TLR4$	$\frac{d(TLR4)}{dt} = k_{51} - k_{52} \cdot TLR4 - k_{53} \cdot LPS \cdot TLR4 + k_{54} \cdot LPS\_TLR4$	1000	Toll-like receptor 4
LPS_TLR4	$\frac{d(LPS\_TLR4)}{dt} = k_{53} \cdot LPS \cdot TLR4 - k_{54} \cdot LPS\_TLR4 - \frac{k_{55} \cdot LPS\_TLR4}{Kd_{51} + LPS\_TLR4}$	0	LPS-occupied TLR4
IgM_mRNA	$\frac{d(IgM\_mRNA)}{dt} = \frac{k_{61}}{1 + Pax5^2/Kd_{61}^2 + Bach2^2/Kd_{62}^2 + TCDD\_AhR/Kd_{63}} - k_{62} \cdot IgM\_mRNA$	0.005	IgM mRNA
IgM	$\frac{d(IgM)}{dt} = k_{63} \cdot IgM\_mRNA - k_{64} \cdot IgM$	2.3	IgM protein
$IgMs$	$\frac{d(IgMs)}{dt} = k_{64} \cdot IgM$	0	Secreted IgM

Note: Initial values represent the steady-state values associated with the B cell state in the deterministic model. For stochastic simulations, these values were rounded to the nearest integers to represent the initial copy numbers of the variables at the beginning of each simulation. For both deterministic and stochastic simulations, the model was first run from these assigned initial conditions for at least 200 hours to ensure steady state is first reached before any LPS and/or TCDD exposure was applied.

Unless otherwise indicated, the unit of abundance used for molecular species (state variables) is number of molecules per cell. For simplicity, IgM, which consists of several subunits, was modeled as a single entity. To generate model-simulated IgM histograms, it was assumed that ten IgM molecules in a simulated cell produce one arbitrary unit of fluorescence intensity. Background fluorescence was assumed to follow a log-normal distribution (with mean=1.5 and variance=1 for the associated normal distribution). For each simulated cell, a number drawn randomly from this distribution was added to the computed IgM fluorescence intensity to obtain total fluorescence intensity. Fifty bins were used to plot simulated IgM histograms. A simulated cell was counted as IgM^{high} if its intracellular IgM level was above 100 (equivalent to ten units of fluorescence intensity).

Table S2. Default parameter values of the computational model

Parameter	Value	Note
k_{00}	0.042 (s^{-1})	Basal deactivation rate constant of Bcl6 gene
k_{01}	39.3 (s^{-1})	Prdm1-dependent deactivation rate constant of Bcl6 gene
k_{02}	0.01 (s^{-1})	Activation rate constant of Bcl6 gene
k_{03}	0.0425 (s^{-1})	Transcription rate constant of Bcl6 mRNA
k_{04}	1.93e-4 (s^{-1})	Degradation rate constant of Bcl6 mRNA
k_{05}	6.0e-4 (s^{-1})	Translation rate constant of Bcl6 protein
k_{06}	9.65e-5 (s^{-1})	Degradation rate constant of Bcl6 protein
k_{10}	6.5e-5 (s^{-1})	Basal activation rate constant of Prdm1 gene
k_{11}	0.082 (s^{-1})	Deactivation rate constant of Prdm1 gene. Since in the current model Prdm1 is repressed by Bach2 which was absent in our previous model [1], this parameter was adjusted so that Prdm1 protein maintains the same steady-state levels as in our previous model.
k_{12}	2.01 (s^{-1})	AP-1-dependent activation rate constant of Prdm1 gene
k_{13}	0.012 (s^{-1})	Transcription rate constant of Prdm1 mRNA
k_{14}	1.93e-4 (s^{-1})	Degradation rate constant of Prdm1 mRNA
k_{15}	6.0e-4 (s^{-1})	Translation rate constant of Prdm1 protein
k_{16}	1.93e-4 (s^{-1})	Degradation rate constant of Prdm1 protein
k_{20}	0.042 (s^{-1})	Basal deactivation rate constant of Pax5 gene
k_{21}	39.3 (s^{-1})	Prdm1-dependent deactivation rate constant of Pax5 gene
k_{22}	0.01 (s^{-1})	Activation rate constant of Pax5 gene
k_{23}	0.0425 (s^{-1})	Transcription rate constant of Pax5 mRNA
k_{24}	1.93e-4 (s^{-1})	Degradation rate constant of Pax5 mRNA
k_{25}	6.0e-4 (s^{-1})	Translation rate constant of Pax5 protein
k_{26}	9.65e-5 (s^{-1})	Degradation rate constant of Pax5 protein
k_{31}	4.02e-3 (s^{-1})	Maximal production rate of AP-1
k_{32}	8.04e-6 (s^{-1})	Degradation rate constant of AP-1
k_{33}	1.25e-3 (s^{-1})	Dephosphorylation rate constant of AP-1p
k_{34}	3.146e-4 (s^{-1})	Basal phosphorylation rate constant of AP-1
k_{35}	5.9e-6 (s^{-1})	LPS_TLR4-dependent phosphorylation rate constant of AP-1
k_{36}	8.04e-6 (s^{-1})	Degradation rate constant of AP-1p
k_{41}	8e-4 ($nM^{-1}s^{-1}$)	Association rate constant for TCDD and AhR binding. This parameter was adjusted to horizontally shift the simulated TCDD concentration-response to make it fit the experimental data as shown in Fig. 8D. k_{41} and k_{42} together give rise to a dissociation constant of 2.5 nM for TCDD and AhR binding, which is in line with the reported range of 0.8 – 14 nM [2-4].
k_{42}	2.0e-3 (s^{-1})	Dissociation rate constant for TCDD_AhR
k_{51}	1.93e-3 (s^{-1})	Basal production rate of TLR4
k_{52}	1.93e-6 (s^{-1})	Degradation rate constant of TLR4
k_{53}	2.08e-4 ($ml \cdot \mu g^{-1}s^{-1}$)	Association rate constant for LPS and TLR4 binding
k_{54}	1.0e-4 (s^{-1})	Dissociation rate constant for LPS_TLR4
k_{55}	7.0e-3 (s^{-1})	Maximal degradation rate of LPS_TLR4. This parameter, together with Kd_{51}, determines how soon TLR4 is downregulated after LPS binding. It was adjusted to make the model-generated dynamic of IgM^{high} cell response to LPS fit the experimental data as shown in Fig. 3D.
k_{61}	4.72e-4 (s^{-1})	Maximal transcription rate of IgM mRNA. This parameter and k_{63} were collectively adjusted to meet two conditions: (1) the average

		IgM level in a plasma cell is about 1000, and (2) the stochastic fluctuation of IgM can give rise to sufficient variability of IgM content in plasma cells that is comparable to the experimental data as shown in Figs. 3, 4, and 8.
k_{62}	1.93e-4 (s^{-1})	Degradation rate constant of IgM mRNA. A half-life of 1 h is assumed for IgM mRNA.
k_{63}	0.0834 (s^{-1})	Translation rate constant of IgM protein. See rationale for k_{61}.
k_{64}	1.93e-4 (s^{-1})	Secretion rate constant of IgM protein. It is assumed that mature IgM molecules are relatively stable in the cell, such that they are primarily cleared from the cell through the secretory pathway. Cells are assumed to empty half of their IgM contents in an hour.
k_{71}	0.01 (s^{-1})	Deactivation rate constant of Bach2 gene. The value is assumed.
k_{72}	7.31e-3 (s^{-1})	Pax5-dependent activation rate constant of Bach2 gene. This parameter is adjusted such that in the plasma cell state the level of Bach2 is at 3, the same as other repressors such as Pax5 and Bcl6.
k_{73}	0.0425 (s^{-1})	Transcription rate constant of Bach2 mRNA. This parameter is set at the same value as for other repressors such as Bcl6 and Pax5.
k_{74}	1.93e-4 (s^{-1})	Degradation rate constant of Bach2 mRNA. This parameter is set at the same value as for other repressors such as Bcl6 and Pax5.
k_{75}	6e-4 (s^{-1})	Translation rate constant of Bach2 protein. This parameter is set at the same value as for other repressors such as Bcl6 and Pax5.
k_{76}	9.65e-5 (s^{-1})	Degradation rate constant of Bach2 protein. This parameter is set at the same value as for other repressors such as Bcl6 and Pax5.
a_{11}	0.75	Weighing factor of Pax5-dependent repression of Prdm1
a_{12}	0.25	Weighing factor of Bach2-dependent repression of Prdm1. The ratio of a_{12} to a_{11} was adjusted so that when Bach2 gene is deleted, the IgM^{high} cell response to 0.45 μg/ml LPS increases from ~15% to ~55% (Fig. 6B), a result that is comparable to the enhanced plasma cell production observed with splenic B cells from $Bach2^{-/-}$ mice compared to $Bach2^{+/+}$ mice [5].
a_{71}	4	AhR-dependent activation rate constant of Bach2 gene. The current value, together with Kd_{72}, allows Bach2 to be induced to a bit over 2-fold by 10 nM TCDD in B cells, a change that is comparable to the 1.5-3 fold we observed experimentally in CH12.LX cells [6].
Kd_{01}	1000	Dissociation constant of Prdm1 binding to Bcl6 promoter
Kd_{11}	150	Dissociation constant of Pax5 binding to Prdm1 promoter
Kd_{12}	1.11	Inhibition constant of Bcl6 repressing AP-1 transcriptional activity
Kd_{13}	1e4	Dissociation constant of AP-1 binding to Prdm1 promoter
Kd_{14}	150	Dissociation constant of Bach2 binding to Prdm1 promoter. Assumed to be the same as Kd_{11}, the dissociation constant of Pax5 binding to Prdm1 promoter.
Kd_{21}	1000	Dissociation constant of Prdm1 binding to Pax5 promoter
Kd_{31}	2.5e4	Inhibition constant of TCDD_AhR repressing AP-1 production. This parameter was adjusted so that along with the Bach2 and IgH pathways active, the IgM^{high} cell response is maximally suppressed to about 1/3 of the control as we demonstrated in the present study (Fig. 8) and reported previously [1, 7-9].
Kd_{51}	50	Michaelis-Menten constant of saturable LPS_TLR4 degradation
Kd_{61}	18	Inhibition constant of Pax5 repressing IgM gene transcription. This parameter and Kd_{62} together determine that the high Pax5 and Bach2 levels at the B cell state repress IgM to a basal level slightly above 2.

Kd_{62}	18	Inhibition constant of Bach2 repressing IgM gene transcription. See rationale for Kd_{61}
Kd_{63}	1.7e5	Inhibition constant of TCDD_AhR repressing IgM gene transcription. This value accounts for a small (5%) direct repression of IgM production by saturating TCDD.
Kd_{71}	2000	Dissociation constant of Pax5 binding to Bach2 promoter. Assumed to be at a relatively high value compared to the amount of Pax5, such that the repression of Bach2 by Pax5 is mostly in a linear range.
Kd_{72}	2e4	Dissociation constant of TCDD_AhR binding to Bach2 promoter. See rationale for a_{71}.
AhR_{tot}	1e4	Total abundance of AhR
$Bach2\_GENE_{tot}$	2	Total abundance of Bach2 gene. Two copies were assumed.
$Bcl6\_GENE_{tot}$	2	Total abundance of Bcl6 gene
$Prdm1\_GENE_{tot}$	2	Total abundance of Prdm1 gene
$Pax5\_GENE_{tot}$	2	Total abundance of Pax5 gene
LPS	0 (µg/ml)	LPS concentration
$TCDD$	0 (nM)	TCDD concentration

References

1. Zhang, Q., S. Bhattacharya, D.E. Kline, R.B. Crawford, R.B. Conolly, R.S. Thomas, N.E. Kaminski, and M.E. Andersen, *Stochastic modeling of B lymphocyte terminal differentiation and its suppression by dioxin.* BMC Syst Biol, 2010. **4**: p. 40.
2. Roberts, E.A., P.A. Harper, J.M. Wong, Y. Wang, and S. Yang, *Failure of Ah receptor to mediate induction of cytochromes P450 in the CYP1 family in the human hepatoma line SK-Hep-1.* Arch Biochem Biophys, 2000. **384**(1): p. 190-8.
3. Roberts, E.A., K.C. Johnson, and W.G. Dippold, *Ah receptor mediating induction of cytochrome P450IA1 in a novel continuous human liver cell line (Mz-Hep-1). Detection by binding with [3H]2,3,7,8-tetrachlorodibenzo-p-dioxin and relationship to the activity of aryl hydrocarbon hydroxylase.* Biochem Pharmacol, 1991. **42**(3): p. 521-8.
4. Roberts, E.A., K.C. Johnson, P.A. Harper, and A.B. Okey, *Characterization of the Ah receptor mediating aryl hydrocarbon hydroxylase induction in the human liver cell line Hep G2.* Arch Biochem Biophys, 1990. **276**(2): p. 442-50.
5. Muto, A., K. Ochiai, Y. Kimura, A. Itoh-Nakadai, K.L. Calame, D. Ikebe, S. Tashiro, and K. Igarashi, *Bach2 represses plasma cell gene regulatory network in B cells to promote antibody class switch.* EMBO J, 2010. **29**(23): p. 4048-61.
6. De Abrew, K.N., A.S. Phadnis, R.B. Crawford, N.E. Kaminski, and R.S. Thomas, *Regulation of Bach2 by the aryl hydrocarbon receptor as a mechanism for suppression of B-cell differentiation by 2,3,7,8-tetrachlorodibenzo-p-dioxin.* Toxicol Appl Pharmacol, 2011. **252**(2): p. 150-8.
7. Tucker, A.N., S.J. Vore, and M.I. Luster, *Suppression of B cell differentiation by 2,3,7,8-tetrachlorodibenzo-p-dioxin.* Mol Pharmacol, 1986. **29**(4): p. 372-7.
8. Schneider, D., M.A. Manzan, R.B. Crawford, W. Chen, and N.E. Kaminski, *2,3,7,8-Tetrachlorodibenzo-p-dioxin-mediated impairment of B cell differentiation involves dysregulation of paired box 5 (Pax5) isoform, Pax5a.* J Pharmacol Exp Ther, 2008. **326**(2): p. 463-74.
9. North, C.M., B.S. Kim, N. Snyder, R.B. Crawford, M.P. Holsapple, and N.E. Kaminski, *TCDD-mediated suppression of the in vitro anti-sheep erythrocyte IgM antibody forming cell response is reversed by interferon-gamma.* Toxicol Sci, 2009. **107**(1): p. 85-92.